Evolution of the bulk optical properties of bovine muscles during wet aging

Robbe Van Beers [a,*], Mito Kokawa [a,b], Ben Aernouts [a,c], Rodrigo Watté [a], Stefaan De Smet [d], Wouter Saeys [a]

[a] *KU Leuven, Department of Biosystems, MeBioS, Kasteelpark Arenberg 30, 3001 Leuven, Belgium*
[b] *Analytical Science Division, National Food Research Institute, National Agriculture and Food Research Organization, 2-1-12 Kan-nondai, Tsukuba, Ibaraki 305-8642, Japan*
[c] *KU Leuven, Department of Microbial and Molecular Systems, Cluster for Bioengineering Technology, Campus Geel, Kleinhoefstraat 4, 2440 Geel, Belgium*
[d] *Ghent University, Department of Animal Production, Laboratory for Animal Nutrition and Animal Product Quality (LANUPRO), B-9090 Melle, Belgium*
** Email: wouter.saeys@kuleuven.be*
Tel: +32 (0) 16 37 71 32
Fax: +32 (0) 16 32 19 94

Abstract

The bulk optical properties (BOP) of two bovine muscles were studied in the 500 nm to 1850 nm wavelength range. Over a two-week period of wet aging, the BOP of the *biceps femoris* (BF) and *longissimus lumborum* (LL) were determined and related to moisture content, tenderness and cooking loss. The absorption by myoglobin and reduced scattering coefficient were higher in the BF compared to the LL. The scattering anisotropy factor was relatively high (>0.95 for LL), representing dominant forward scattering. Two-toning effects in the BF could be attributed to significant scattering differences, as no differences in absorption properties were observed. During wet aging, the anisotropy factor decreased, while tenderness increased. It was hypothesized that this might be related to proteolysis of cytoskeletal proteins. The results show the potential use of BOP to monitor tenderization and the cause of color differences in beef muscles. Moreover, this information could be used to develop and optimize optical sensors for non-destructive meat quality monitoring.

Keywords: Meat quality, Scattering, Absorption, Anisotropy factor, Double integrating spheres, Unscattered transmittance

1. Introduction

The meat industry aims for reliable meat quality monitoring throughout the production process in order to guarantee a high quality of the final product (Damez & Clerjon, 2008; Troy & Kerry, 2010). Nevertheless, large variability in the muscle type and quality often results in a highly variable end product (Damez & Clerjon, 2013). For this reason, the meat sector is interested in technology for accurate, fast and non-destructive determination of quality attributes. Both chemical (pH, color and fat content) and physical parameters (tenderness and juiciness) contribute to the meat appearance and eating experience and, therefore, to the final consumer acceptability.

Optical sensors provide a fast way to non-destructively measure food products. Optical techniques such as vis/NIR spectroscopy (Prieto et al., 2009; Ripoll et al., 2008), spatially and time resolved spectroscopy (Swartling et al., 2003; Xia et al., 2007) and hyperspectral imaging (Elmasry et al., 2012) have been studied to measure quality attributes of many food products, including meat (Nicolaï et al., 2014; Prieto et al., 2009). These methods measure the light which interacted with the sample of interest and which is reflected in the direction of the sensor. The obtained reflectance signals are affected by both the chemical and physical properties of the sample, which are responsible for respectively the absorption and scattering of the propagating light photons (MacDougall, 1982; Nicolaï et al., 2007; Swatland, 1991).

Light scattering in biological tissue is typically caused by local non-uniformities in the physical microstructure. The intensity and the direction of the light scattering depend on the size, the shape and the refractive index-mismatch of the scattering particles (Nicolaï et al., 2007; Peng & Dhakal, 2015). These non-uniformities can be cell organelles, fibrous structures, air pores,…. The light deflections determine the path length of the photons traveling through the sample (López-Maestresalas et al., 2015). As the chance for a photon to be absorbed in a medium with a given concentration of a certain chromophore is proportional to the photon's

path length travelled in this medium (cf. Beer-Lambert law), the effects of absorption and scattering are indissolubly connected in the obtained optical measurements (Van Beers et al., 2015). Accordingly, changes in the scattering properties of the sample, altering the photon path length, might be misread as a change in the absorption, related to the composition.

The propagation of light in turbid media, like biological materials, can be described by the radiative transport theory (RTT) which considers the tissue's bulk optical properties (BOP). These BOP include the bulk absorption coefficient μ_a, the bulk scattering coefficient μ_s and the angular scattering pattern, represented by the normalized scattering phase function $p(\theta)$ (Tuchin, 2007). This phase function describes the normalized scattering probability as a function of the scattering angle θ, but is often too complex to interpret. Therefore, the mean cosine of the scattering angle, called the anisotropy factor g, is generally used instead. This wavelength dependent parameter describes the scattering direction with values ranging from isotropic Rayleigh scattering ($g = 0$) to complete forward scattering ($g = 1$). In most biological tissues, an anisotropy factor close to 1 is found, indicating high forward scattering (Aernouts et al., 2015; Tuchin, 2007). As it is not always possible to estimate the scattering anisotropy, the bulk scattering coefficient and the anisotropy factor are often combined in a lumped parameter, known as the reduced scattering coefficient μ_s' (Tuchin, 2007).

For determining the BOP of biological tissues, double integrating spheres (DIS) systems are considered to be the 'golden standard' (Aernouts et al., 2013; Bashkatov, 2005; López-Maestresalas et al., 2015; Saeys, 2008; Tuchin, 2007; Zamora-Rojas et al., 2013). By measuring a thin sample slab *in vitro* in-between two integrating spheres, the total reflectance and transmittance can be determined. These measures can then be used to obtain an accurate estimate for μ_a and μ_s' through inversion of light propagation models based on radiative transfer theory. By also measuring the unscattered transmittance (UT) of the sample, the bulk extinction coefficient μ_t can be retrieved. Accordingly, the bulk scattering

coefficient μ_s and the anisotropy factor g can be calculated from μ_a, μ_s' and μ_t (Aernouts et al., 2013; López-Maestresalas et al., 2015; Prahl, 2011).

In the past, the BOP of many agro-food products have been characterized using integrating sphere systems to study their relation with the chemical and physical quality attributes of these products. For example, the BOP of onions (Wang & Li, 2013), apples (Rowe et al., 2014; Saeys et al., 2008; Van Beers, Aernouts, Watté, et al., 2017), milk (Aernouts et al., 2015), potatoes (López-Maestresalas et al., 2015) and pig adipose tissue (Zamora-Rojas et al., 2013) have been measured. The results of these studies have been used as input parameters for simulation purposes, in order to develop novel optical sensors for online or inline quality monitoring (Watté et al., 2016; Zamora-Rojas et al., 2014). However, few reports were found on the measurement of the BOP of bovine muscle tissue. Xia *et al.* (2007, 2008) used a spatially resolved spectroscopy setup in combination with a fitting procedure based on the diffusion equation to obtain the absorption and reduced scattering coefficient spectra of different beef samples. Zijp & ten Bosch (1998) estimated the anisotropy factor and bulk scattering coefficient spectrum for a single bovine muscle. However, both studies only covered a wavelength region between 380 nm and 950 nm, while many important chemical components (fatty acids, proteins, water, etc.) have their major NIR absorption at wavelengths above 1000 nm. Flock *et al.* (1987) measured the total attenuation coefficient and scattering phase function at a wavelength of 633 nm. To the best of our knowledge, there are no studies reporting the BOP of bovine meat samples for wavelengths above 1000 nm. Moreover, the used DIS setup in this study provides accurate estimates of the BOP values over a large part of the vis/NIR range of the spectrum, even for strongly scattering and absorbing samples (Aernouts et al., 2013). Besides estimating the bulk absorption coefficient and the reduced scattering coefficient, also the anisotropy factor and bulk scattering coefficient can be accurately determined.

Therefore, the main goal of this study was to provide accurate estimations of μ_a, μ_s, μ_s' and g for two bovine muscles from 500 nm to 1850 nm and the way in which these properties change during wet aging. A DIS setup in combination with a measurement of the unscattered transmittance was used to obtain accurate estimates for the BOP.

2. Materials and methods

2.1 Muscle samples

Two bovine muscles, *longissimus lumborum* (LL) and *biceps femoris* (BF), were collected at a commercial meat handling facility in Belgium (Hemelaer-NV, Opwijk, Belgium). Both muscles were sampled the day after slaughter and originated from one Belgian Blue bull with an age of 19.5 months and a carcass weight at slaughter of 503 kg. Of each muscle, a total of six samples (size 20 cm x 10 cm x 2.5 cm) were collected and immediately vacuum packed. For the BF muscle, a high intramuscular variability was expected due to the existence of two-toning, induced by heat shortening (Pastsart et al., 2011; Pastsart et al., 2013). Therefore, one sample of the outer BF (OBF) and one sample of the inner BF (IBF) were used per week for the wet aging experiment. Hence, in the current study, a total of six LL samples, three OBF samples and three IBF samples were considered. All the samples were stored in a refrigerator (4°C) during the wet aging process. After one day, one week and two weeks of wet aging, each time two LL samples, one IBF and one OBF sample were unpacked. After unpacking, subsamples were taken to perform optical measurements (section 2.2) and reference quality measurements (section 2.3).

2.2 Meat bulk optical properties

2.2.1 Double integrating spheres (DIS) and unscattered transmittance (UT) setup

To determine the BOP of the muscle tissue samples, a double integrating spheres (DIS) setup in combination with a measurement of the unscattered transmittance (UT), described by Aernouts *et al.* (2013), was used. Samples were placed in a sample holder which was located between two *Infragold*® coated integrating spheres (RT-060-IG, Labsphere Inc., North Sutton, USA). The light collected by the detectors on the sphere in front of the sample and by the sphere on the backside of the sample is a measure for respectively the total reflectance (M_R) and the total transmittance (M_T). In a separate measuring path, the unscattered transmittance (M_u) of the sample was determined. For this, the sample was placed in a sample holder with the detectors positioned at a large distance (1.5 m) behind the sample. In this way, the contribution of scattered photons to the measurement was limited. A supercontinuum laser (SC450-4, Fianium Ltd., Southampton, UK) in combination with a monochromator (Oriel Cornerstone 260 ¼ m, Newport, Irvine, USA) was used as a tunable monochrome illumination source. The wavelength of the illumination beam was varied from 500 nm to 1850 nm in steps of 5 nm. To measure the different spectra (M_R, M_T and M_U), a Si detector (PDA100A, Thorlabs Inc., Newton, NJ, USA) and a one-stage Peltier-cooled extended-InGaAS detector (PDA10DT-EC, Thorlabs Inc., Newton, NJ, USA) were used for wavelengths below and above 1050 nm, respectively.

All the detectors in the setup were read by a data acquisition card (NI PCI-6251, National Instruments Corporation, TX, USA), while the measurement procedure was programmed in LabView 8.5 (National Instruments Corporation, Austin, TX, USA). More details about the DIS and UT measurement setup can be found in Aernouts *et al.* (2013).

2.2.2 Sample preparation and measurements

Before the meat samples could be measured with the DIS/UT setup, an extensive sample preparation was required. A thin sample slab was needed to ensure sufficient total and unscattered transmission signals. Therefore, two small subsamples of about 3.5 cm x 3.5 cm x 1 cm were cut from the original unpacked sample. These subsamples were embedded in

161 an optimal cutting temperature compound (OCT Compound 361603E, VWR International,
162 Radnor, PA, USA) without incorporating air bubbles, as these might cause cracks during
163 freezing. Next, the subsamples were indirectly frozen by putting them in a metal cup
164 submerged in liquid nitrogen. This indirect contact with the liquid nitrogen ensured that the
165 subsample froze without forming cracks. Subsequently, the subsamples were stored at -80°C
166 until the end of the wet aging period (Mager et al., 2007). After all the subsamples had been
167 collected and frozen, they were cut into slices of 0.5 mm using a microtome-cryostat (Microm
168 HM 560 Cryostat, Thermo Fisher Scientific, Waltham, MA, USA). The slicing was performed
169 perpendicular to the muscle fiber orientation. For the IBF and OBF sample, two slices per
170 subsample were obtained, while for the LL muscle samples, only one slice per subsample
171 was retained. The obtained slices were cut into round disks of 30 mm diameter and placed in
172 a custom-made glass cuvette. This cuvette consisted of two parallel 1.1 mm thick glass
173 plates (Borofloat33, Schott, Germany) separated by a 0.55 mm spacer, as described by
174 Aernouts *et al.* (2013). The spacer had a circular hole with a diameter of 30 mm, in which the
175 sample fitted. Before and after positioning the sample slab in the cuvette, demineralized
176 water was added to remove unwanted air bubbles and to reduce refractive index mismatches
177 at the boundaries between the glass plates and the sample (Van Beers, Aernouts, Watté, et
178 al., 2017). The cuvette thickness was measured in triplicate for each sample individually.
179 Finally, the cuvette filled with the sample slab was sequentially placed in the sample holder
180 of the DIS and the UT path to acquire the total reflectance (M_R), the total transmittance (M_T)
181 and the unscattered transmittance (M_U) spectra.

182 *2.2.3 Calculating the bulk optical properties*

183 After performing the DIS (M_R, M_T) and UT (M_U) measurements on the different meat samples,
184 the BOP were estimated using the inverse adding doubling (IAD) routine developed and
185 optimized by Prahl *et al.* (1993). Next to the M_R, M_T and M_U measurements, also the
186 refractive index of the meat samples was required as an input parameter for the IAD routine.
187 As water represents up to 75% of the total fresh matter in meat, the sample refractive index

188 was expected to be close to the refractive index of water (Prieto et al., 2009). Accordingly,
189 the wavelength-dependent real refractive index of water was adopted from Hale & Querry
190 (1973) and a wavelength-independent constant was added. Dirckx *et al.* (2005) found a
191 bovine muscle refractive index of 1.382 ± 0.004 at 592 nm, while the refractive index of water
192 at this wavelength is 1.333 (Hale & Querry, 1973). Based on these findings, a constant of
193 0.049 was added to the refractive index of water for all wavelengths. Besides the sample's
194 refractive index, several setup- and sample-related input parameters were required. For
195 these parameters, like the reflectance efficiency of the sphere wall and the diameter of the
196 illumination beam, the values reported by Aernouts *et al.* (2013) were used.

197 To avoid unwanted air bubbles and to reduce refractive index mismatches at the boundaries
198 between the glass plates and the sample, water was added to the sample. The effect of the
199 added water on the obtained measurements was corrected for in the estimation of the BOP.
200 To this end, a perfect two-layered water-sample system was assumed. The procedure to
201 correct for the effect of the water layer is described in detail by Van Beers *et al.* (2017). It
202 involves calculation of the thickness of the water layer by subtracting the thickness of both
203 glass-walls of the cuvette and the thickness of the sample from the total thickness of the
204 cuvette.

205

206 All data processing steps, among which the estimation of the BOP through the IAD routine,
207 were performed in Matlab (version 7.10, The Mathworks Inc., Natick, MA, USA). To test
208 whether the mean BOP values differed significantly between the different muscle types, an
209 analysis of variance (1-way ANOVA) per wavelength in combination with a Tukey multiple
210 comparison test was performed in Matlab. For all tests, a significance level of 5% was used
211 (p-value = 0.05).

212

2.3 Meat quality measurements

Destructive reference measurements were performed to determine relevant quality parameters and to monitor them during the wet aging period. First, the total moisture content of the samples was determined in triplicate according to the AOAC Method 950.46 (Leffler et al., 2008). To do so, 8-10 g of raw minced sample (corresponding to about 2 g of dry material) was dried for 16 to 18 hours at 102°C in a hot air oven. Before and after drying, the sample was weighted (Adventurer Pro AV412, OHAUS Corporation, Parsippany, NJ, USA) in order to determine the total moisture content.

Tenderness was evaluated according to the Warner-Bratzler shear force (WBSF) method described by Boccard *et al.* (1981). After collecting sub-samples (for DIS/UT measurements and moisture content determination) from each meat sample, the remaining part was weighed and placed in a thin-walled polyethylene bag. The bag was placed in a water bath (Grant GR150, Grant Instruments Ltd, Shepreth, Cambridgeshire, UK) at 75°C for 50 minutes, to make sure that the meat center reaches this temperature (Boccard et al., 1981). Next, the packed sample was cooled for 40 minutes using running tap water. After cooling, the sample was unpacked and weighed again to determine the cooking loss, after which it was placed in a refrigerator at 4°C overnight. As only one sample of both the OBF and IBF were used every aging time, no replicates were possible. For the LL muscle, two samples per aging time were measured. For each meat sample, 10 cylindrical cores (diameter of 1.25 cm) parallel to the muscle fiber direction were taken to use in the Warner-Bratzler shear force (WBSF) measurement. The maximum force which is needed to press a V-shaped cutting blade (60° V-notch) through the meat cylinder was measured with a universal testing machine (Type LS1 Material Tester, LLoyd materials testing, West Sussex, UK). This measurement was repeated for 10 cylinders per meat sample, and the mean maximum force value is considered the WBSF value. Higher WBSF values correspond to lower meat tenderness (Gruber et al., 2006).

To test whether the mean values of the measured quality traits (total moisture content, cooking loss and tenderness) differed significantly between the muscle types and between days postmortem (2, 9 and 16 days pm), an analysis of variance (2-way ANOVA) in combination with a Tukey multiple comparison test was performed in Matlab.

3. Results and Discussion

3.1 Meat quality measurements

In Table 1 the results of the meat quality measurements are shown according to muscle type and aging time.

Table 1 Mean values ± standard deviation for water content (%), cooking loss (%) and Warner-Bratzler shear force (N) during wet aging for the *biceps femoris* (BF) and *longissimus lumborum* (LL) muscles.

		Time postmortem (days)		
	Muscle	**2**	**9**	**16**
WBSF (N)	IBF	31.81 ± 10.00 ^{a}	31.63 ± 9.04 ^{a}	26.06 ± 8.69 ^{a}
	OBF	40.20 ± 13.81 ^{ab}	33.57 ± 7.45 ^{a}	30.63 ± 9.93 ^{a}
	LL	78.46 ± 19.23 ^{c}	56.92 ± 24.90 ^{b}	30.61 ± 8.54 ^{a}
Moisture content (%)	IBF	73.05 ± 0.27 ^{ab}	72.52 ± 0.21 ^{a}	73.06 ± 0.12 ^{ab}
	OBF	72.64 ± 0.13 ^{a}	73.13 ± 0.07 ^{ac}	73.09 ± 0.10 ^{ac}
	LL	74.39 ± 0.41 ^{d}	73.69 ± 0.35 ^{bc}	73.79 ± 0.22 ^{cd}
Cooking loss (%)	IBF	22.85	23.92	26.80
	OBF	25.70	24.08	25.85
	LL	18.22 ± 0.88 ^{a}	27.50 ± 11.10 ^{a}	25.35 ± 0.45 ^{a}

IBF = inner biceps femoris; OBF = outer biceps femoris. Mean values within the same quality trait without a common letter superscript are significantly different at P < 0.05.

As can be noticed from Table 1, a significant decrease in WBSF values appeared during wet aging of the LL muscle. This observation is consistent with the results reported by other researchers (Bratcher et al., 2005; Gruber et al., 2006; Smith et al., 2008; Xia et al., 2008). A

256 decrease in WBSF was also expected in the BF muscle (Gruber et al., 2006). However,
257 although a decrease in the WBSF values of the BF muscle samples in function of the time
258 postmortem can be noticed (Table 1), this effect was not significant. The moisture content of
259 the LL muscle decreased in the period between day 2 and 9 postmortem, after which it
260 slightly increased again. For the BF muscle, on the other hand, no significant differences
261 were noted between the different types (IBF vs. OBF) and days postmortem (Table 1). In
262 contrast to these results, Li *et al.* (2008) found an increase in moisture content of the
263 *semitendinosus* muscle from day 4 to day 14 of wet aging, after which a small decrease was
264 noticed until day 28. In addition, Li *et al.* (2008) also suggested that wet aging resulted in an
265 increase of cooking losses. Nevertheless, other researchers found no clear changes in
266 cooking losses over a five week wet aging period (Jeremiah & Gibson, 2003). In this study,
267 as only a limited number of samples was measured, no significant differences in cooking loss
268 could be identified. Nevertheless, both in the IBF and LL muscle samples, an increasing
269 trend can be noticed from Table 1.

270 ### *3.2 Bulk optical properties of bovine muscles*

271 In Figure 1 the mean value and standard deviation (error bars) for the estimated bulk
272 absorption coefficient (Figure 1a) and reduced scattering coefficient (Figure 1b) are shown
273 for both the LL and BF muscle samples. The separation between the IBF and OBF is shown
274 as well. The mean values and standard deviations were calculated over the total duration of
275 the study (day 2 until day 16 postmortem). For each muscle type considered, this involved 12
276 sample slices

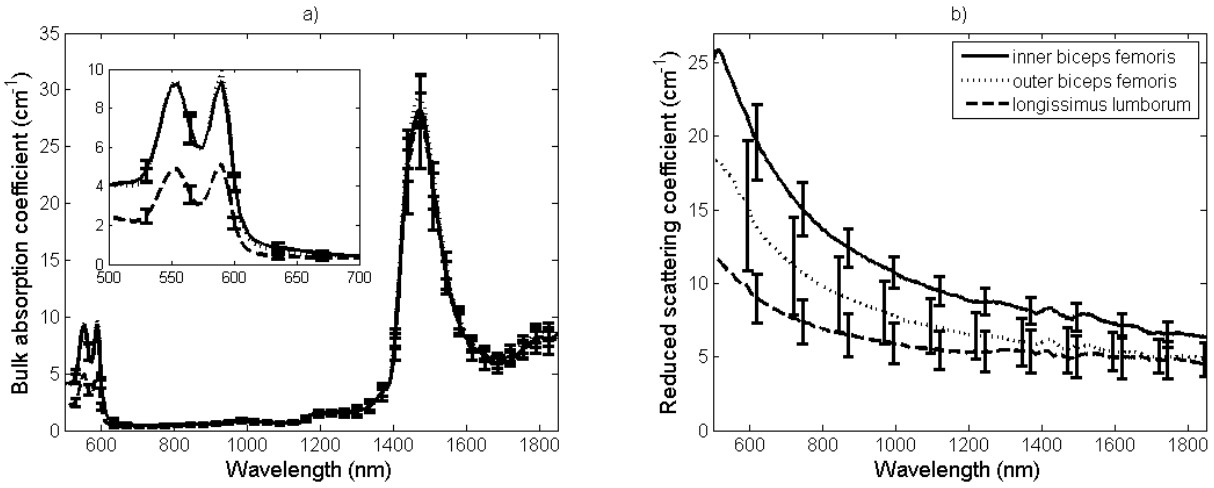

Figure 1 (a) Mean bulk absorption coefficient μ_a and (b) mean reduced scattering coefficient μ_s' of the measured bovine muscles over a two-week wet aging period. The inset figure on the left shows the mean absorption coefficient over a smaller wavelength range from 500 nm to 700 nm. The error bars indicate the standard deviation.

3.2.1 Water and myoglobin dominate the absorption coefficient spectra of muscle tissue

In Figure 1a, some clear absorption features can be observed. Water is one of the main constituents present in muscle tissue and makes up about 75% of the total fresh matter (Prieto et al., 2009) (Table 1). Accordingly, some distinctive absorption peaks can be observed at 970 nm, 1200 nm and 1450 nm, which can be attributed to absorption by the O-H bonds in water. While water is mainly absorbing in the NIR range (700 – 1850 nm), myoglobin is a meat component which absorbs most of the visible light (400 – 700 nm). Myoglobin is an oxygen-binding molecule, which can be present in three different forms: oxymyoglobin, deoxymyoglobin and metmyoglobin (Prieto et al., 2009). Prior to the DIS and UT measurements, the 0.5 mm thick samples were prepared in an aerobic environment. Accordingly, the myoglobin was mainly present in the oxygenated state: oxymyoglobin. The latter has a distinctive dual absorption peak at 544 nm and 582 nm (Cozzolino & Murray, 2004; Millar et al., 1996). These absorption peaks, resulting in a bright red color, are clearly visible in Figure 1a. Apart from these dominant absorbers, also protein and intramuscular fat affect the NIR spectrum due to the absorption by N-H bonds (1460-1570 nm) and C-H bonds (1100-1400 nm and 1700 nm), respectively (Prieto et al., 2009). The vis/NIR absorption coefficient spectra of BF and LL muscles were most different at the absorption region of

300 myoglobin (Figure 1a inset). This variation is most likely related to a different myoglobin
301 concentration in these two muscle types (Rickansrud & Henrickson, 1967; Von Seggern et
302 al., 2005). Moreover, Rickansrud & Henrickson (1967) found a higher total pigment
303 concentration of 4.85 mg/g in the BF muscle compared to 3.97 mg/g for the LL muscle.
304 There was, however, no significant difference in the absorption between the inner and outer
305 BF muscle samples.

306

307 *3.2.2 Higher scattering explains the lighter color of the inner biceps femoris muscle*

308 The scattering behavior in the muscles is illustrated in Figure 1b, showing the mean reduced
309 scattering coefficient calculated over the total duration of the study (day 2 until day 16
310 postmortem). From this figure, a clear decreasing trend can be observed with increasing
311 wavelength, which is typical for biological tissues (Bashkatov et al., 2005; Jacques, 2013). At
312 all wavelengths, a significantly higher μ_s' was found for the lBF samples compared to the
313 OBF and the LL samples, while the μ_s' of the OBF sample was only significantly higher than
314 the LL muscle for wavelengths below 1175 nm.

315

316 In Figure 2, the measured μ_s' spectra of the LL muscle are compared to the values obtained
317 by Xia *et al.* (2008) over a much smaller wavelength range (600 nm to 950 nm).

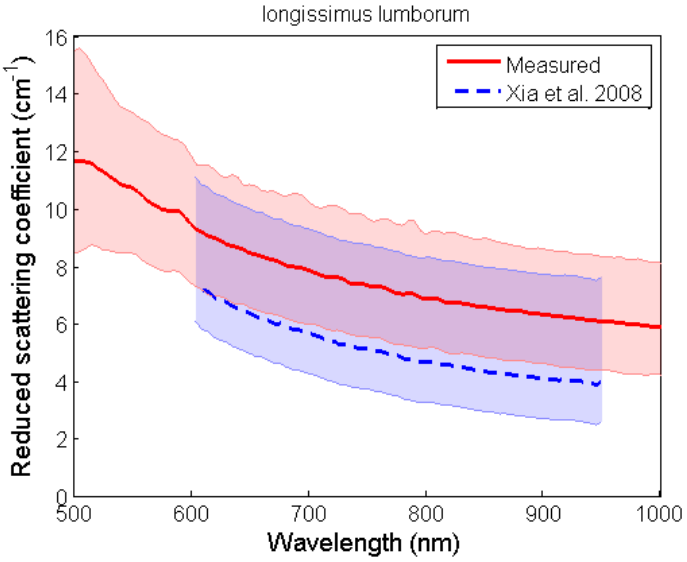

Figure 2 Comparison of the reduced scattering coefficient in the 500 to 1000 nm range measured for the *longissimus lumborum* sample to the values reported by Xia *et al.* (2008). The lines indicate the mean values both in this study and by Xia *et al.* (2008), while the areas indicate the ranges.

Xia *et al.* (2008) measured four different muscles, including the *longissimus dorsi*, which is a former designation to describe the *longissimus lumborum* (Kauffman, 1990). In Figure 2, a similar magnitude and overall trend of the μ_s' values over the measured wavelength range can be observed although the mean values they reported were somewhat lower. Moreover, the BOP values obtained in this research illustrate the intramuscular variation in a single LL muscle, as multiple samples from the same LL muscle, originating from one bull, were measured. In the μ_s' values reported by Xia *et al.* (2008), the intermuscular variation was captured, as 92 muscles were considered. In their study, the LL μ_s' values ranged from 4 cm^{-1} to 9 cm^{-1} at 721 nm, which is in line with the results obtained in this study. The range of obtained μ_s' values is shown as the blue band in Figure 2. It should be noted that the results in this study were obtained from DIS and UT measurements in combination with an IAD routine, while the results in the work by Xia *et al.* (2008) were derived from measuring the diffuse reflectance at several distances from the point of illumination. The used DIS/UT setup in this study provides a reliable separation between the bulk optical properties, even for strongly scattering and absorbing biological samples (Aernouts et al., 2013; López-Maestresalas et al., 2015; Van Beers, Aernouts, Watté, et al., 2017). Therefore, accurate

estimations of μ_a, μ_s' and the anisotropy factor *g* are obtained. In addition, Xia *et al.* (2008) dry aged the LL muscle samples at 4°C for 1, 7, 14 or 21 days.

In Figure 3a, the bulk scattering coefficient μ_s spectra are shown for the different muscle samples averaged over the entire wet aging period, while Figure 3b shows the anisotropy factor *g*. For each muscle type considered, this involved 12 sample slices collected over the entire wet aging period.

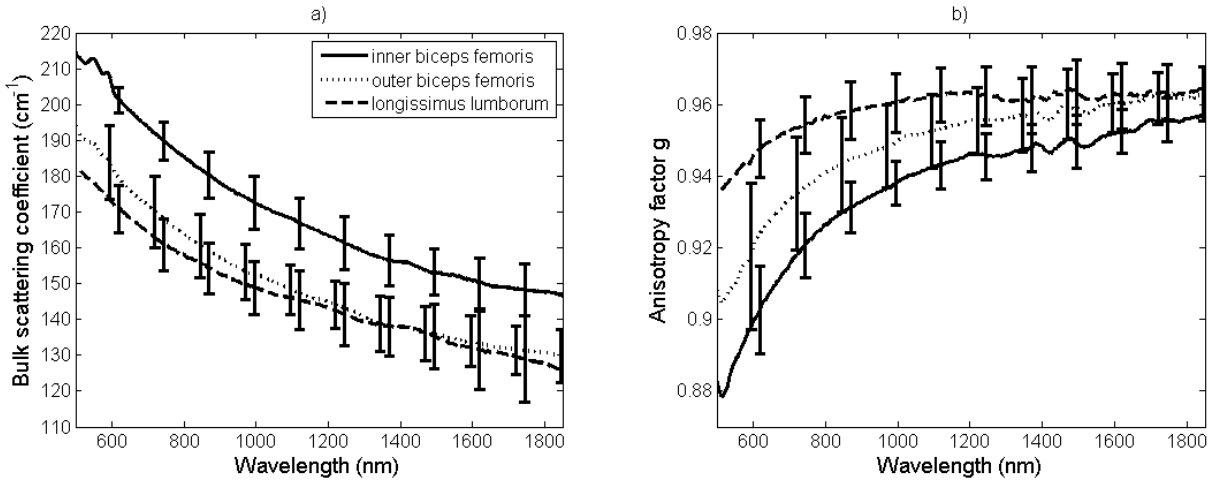

Figure 3 (a) Mean bulk scattering coefficient μ_s and (b) mean anisotropy factor *g* of two bovine muscles measured over a two-week wet aging period. The error bars indicate the standard deviation.

In Figure 3a, a significant difference in the bulk scattering coefficient of the IBF compared to the other muscle samples can be observed for all wavelengths. Additionally, it was found that the bulk scattering coefficient spectra of the OBF were significantly different from those of the LL muscle for wavelengths below 700 nm. The IBF muscle samples had an overall higher μ_s with mean values up to 185 cm^{-1} at 800 nm, while at the same wavelength, the OBF and the LL samples had a mean value of 164 cm^{-1} and 158 cm^{-1}, respectively. For the anisotropy factor *g*, on the other hand, also significant differences between the IBF and LL samples were found over the entire wavelength range. The OBF only showed significant differences with the LL samples below 1195 nm, and with the IBF samples below 1370 nm. For all muscle samples an anisotropy factor close to one was measured, indicating high forward

360 scattering, with a mean *g*-value at 800 nm of 0.927, 0.941 and 0.957 for the IBF, OBF and LL
361 samples, respectively. Moreover, the anisotropy had an increasing trend with increasing
362 wavelengths, typically observed in biological tissues (Jacques, 2013).

363 According to Xia *et al.* (2008), two major structural characteristics influence the scattering
364 properties of muscles: the collagen content and protein-protein interactions within the
365 sarcomere. Rhee *et al.* (2004) showed a significant difference ($p<0.05$) in the collagen
366 concentration between BF and LL, with 8.74±1.12 mg/g for the BF compared to 4.52±0.66
367 mg/g for the LL. Moreover, it was found that the sarcomere length of both muscles is very
368 similar (Rhee et al., 2004). Therefore, a large part of the observed differences in the
369 scattering properties can most likely be attributed to the concentration of collagen.

370 Moreover, as both muscles originated from a different part of the animal, the muscle fiber
371 composition was most likely different (Kirchofer et al., 2002). Both the BF and the LL are
372 categorized as white muscles, mainly consisting of Type IIX muscle fibers. According to
373 Kirchofer et al. (2002), the BF and LL muscles contain respectively 49.3±4% and 43.2±4.4%
374 of Type IIX fibers. Besides this type of muscle fiber, also Type I fibers (21.7±1.9% for the BF
375 to 35±1.4% for the LL) and Type IIa fibers (29±2.3% for the BF to 21.8±3.4% for the LL) are
376 present. Overall, the Type II fibers are thicker in comparison with Type I fibers (Kirchofer et
377 al., 2002). Considering the different diameters and the composition, the overall fiber
378 thickness in BF muscles is smaller than in LL muscles.

379

380 The observed intramuscular scattering difference between the BF samples is most likely
381 related to the effect of two-toning, which has been observed in the BF muscle of Belgian Blue
382 cattle (Pastsart et al., 2011; Pastsart et al., 2013). The obtained results suggest that this
383 visual two-toning effect is caused by differences in the scattering properties rather than in the
384 absorption properties (Figure 1 and Figure 3). The BF intramuscular differences in the
385 amount of scattering could be related to a difference in the amount of protein denaturation.

386 Although not measured in the current study, Pastsart *et al.* (2013) suggested increased
387 protein denaturation in IBF muscle samples of Belgian Blue cattle due to a faster post-
388 mortem pH decline. A similar post-mortem decline in pH is seen in pork muscles, causing
389 pale, soft and exudative (PSE) meat. This PSE meat is related to an increased amount of
390 scattering due to the deposition of denatured sarcoplasmic proteins on the myofibrils
391 (MacDougall, 1982; Swatland, 1994, 2004; Van Oeckel et al., 1999). The increased protein
392 denaturation in the IBF samples might have a similar effect, increasing μ_s (Figure 3a). At the
393 same time, this denaturation of sarcoplasmic proteins might decrease the overall particle
394 size, which results in a decrease in the scattering anisotropy *g* (Figure 3b). According to the
395 Mie scattering theory, a lower anisotropy factor indicates smaller scattering particles (Yavari,
396 2006).

397 Zijp & ten Bosch (1998) also estimated the bulk scattering coefficient and the anisotropy
398 factor of bovine meat samples separately. They measured the *psoas major* at 9 discrete
399 wavelengths between 550 nm and 833 nm and found a mean anisotropy factor around 0.96
400 and a bulk scattering coefficient of 150 cm^{-1}. The anisotropy factor showed an increase from
401 around 0.95 at 550 nm towards 0.97 at 833 nm (Zijp & ten Bosch, 1998). Flock *et al.* (1987)
402 measured the scattering phase function and anisotropy factor *g* of bovine muscle tissue,
403 resulting in a value of 0.954 ± 0.016 for *g* at a wavelength of 632.8 nm. In the current study, a
404 larger wavelength range and different muscles were measured. However, in the wavelength
405 range which they have in common, the obtained results in Figure 3 for the LL muscle are in
406 agreement with the results obtained by both Zijp & ten Bosch (1998) and Flock *et al.* (1987).

407 ### *3.3 Evolution of bulk optical properties during wet aging*

408 So far, the BOP of the muscles were presented after averaging over the entire wet aging
409 period (2 – 16 days postmortem). In Figure 4, the evolution of the measured BOP during this
410 wet aging period is illustrated for some selected wavelengths. The evolution of μ_a is shown at
411 545 nm, corresponding to one of the absorption wavelengths of oxymyoglobin (Figure 1a).
412 The scattering behavior (μ_s, μ_s' and *g*) is shown at 850 nm, as no major absorption features

were present at this wavelength, while this wavelength represents the scattering behavior of the muscles well. Each week measurements were performed on four sample slices per muscle sample, shown as a mean value and standard deviation.

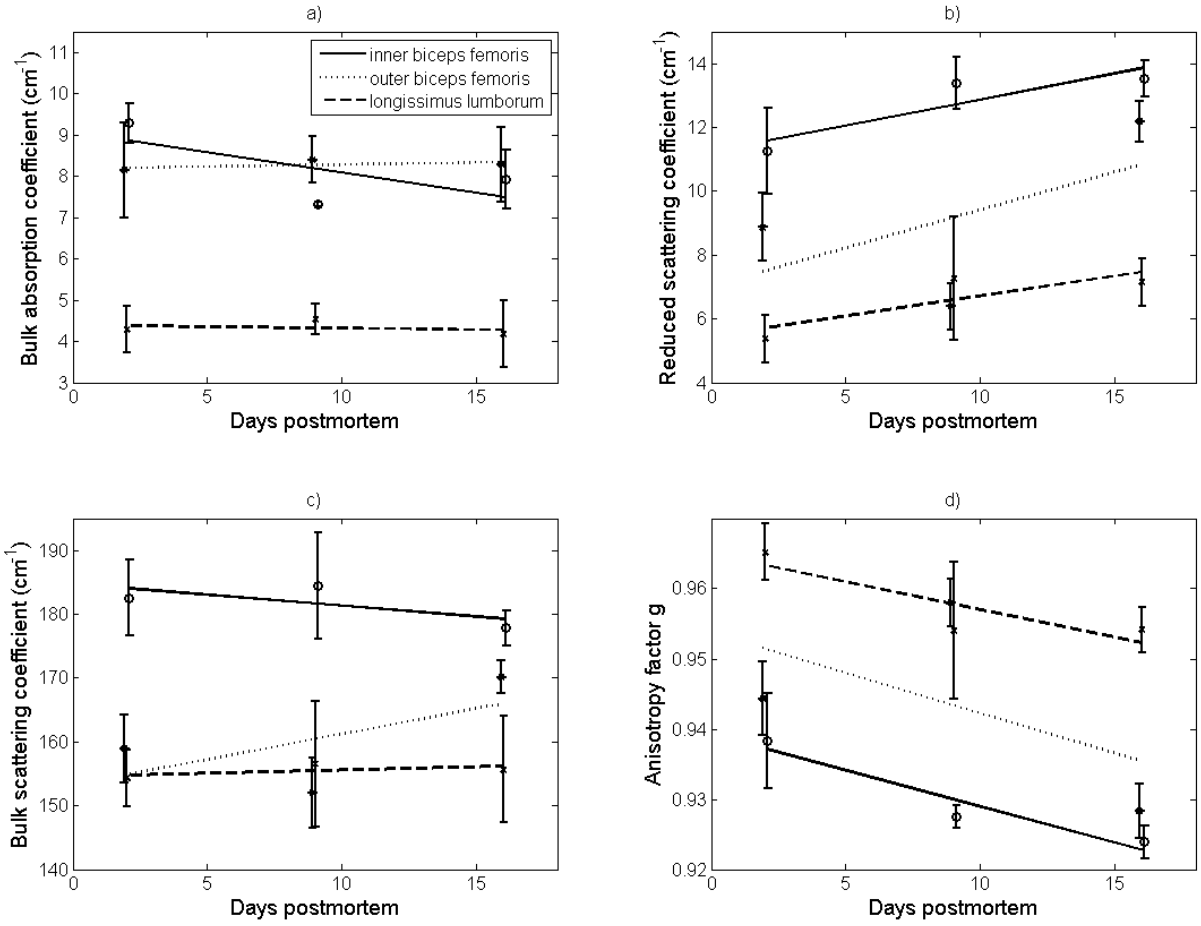

Figure 4 Evolution of the bulk optical properties of two bovine muscles during a two-week wet aging period. (a) The bulk absorption coefficient μ_a, (b) the reduced scattering coefficient μ_s', (c) the bulk scattering coefficient μ_s and (d) the anisotropy factor *g*. The absorption coefficient is shown at a wavelength of 545 nm, while the other optical properties are shown at a wavelength of 850 nm. The error bars indicate the standard deviation.

The decreasing trend of the absorption coefficient at 545 nm (Figure 4a), representing the absorption by myoglobin, was found to be significant in the IBF muscle samples only. This might be related to the higher protein denaturation found in the IBF, as suggested by Pastsart *et al.* (2013). Additionally, it was found that the bulk scattering coefficient did not change significantly during wet aging (Figure 4c). Nevertheless, clear increasing and decreasing trends were observed over time for respectively the reduced scattering coefficient

(Figure 4b) and the anisotropy factor (Figure 4d). For the LL and OBF muscle samples, the increasing trend of the reduced scattering coefficient was found to be non-significant. However, the p-values for these trends were close to 0.05. For the anisotropy factor, only the decreasing trend of the OBF sample was non-significant. Since the bulk scattering coefficient did not change significantly over time, the evolution of the anisotropy factors and the reduced scattering coefficients were negatively correlated.

The significant decreases in the anisotropy factor during the wet aging period could be related to a change in the size and/or shape of the scattering particles. During wet aging, the proteolysis of cytoskeletal proteins is considered the main cause for increasing tenderness (Koohmaraie, 1994; Xia et al., 2008). This process causes the fragmentation of myofibrillar structures in the muscle tissue, which likely affects the overall size of the scattering particles. Xia *et al.* (2008) determined the reduced scattering coefficient of four beef muscles during a 21-day period of dry aging. Their results showed that WBSF was significantly changing the first 7 days of aging, while μ_s' increased during the same period. Our results indicate a similar trend in both WBSF (Table 1) and μ_s' values (Figure 4b) during wet aging, possibly caused by changes in the overall particle size.

4. General discussion

One of the requirements to use the IAD algorithm for the calculation of BOP values from integrating sphere measurements, is that the measured samples are homogeneous (Prahl et al., 1993). However, the measured muscle samples will be more heterogeneous, as for example air pores, color differences, blood vessels and connective tissue can be present. Although this effect on the eventual estimation of optical properties is expected to be limited, a more complex modelling strategy like the meshed Monte Carlo method described by Watté *et al.* (2015) could provide added value in this context. In addition to these possible inconsistencies, muscle tissue is highly anisotropic because of the present muscle fibers, which can affect light propagation (Elliott, 1967; Van Beers, Aernouts, Reis, & Saeys, 2017).

Although the effects of this muscle anisotropy on light propagation have been reported to be clearly present in different types of muscle tissue (Kienle, Foschum, & Hohmann, 2013; Ranasinghesagara & Yao, 2007), the impact of this anisotropy is expected to be limited due to the measurement of thin samples (0.5 mm in thickness). Nevertheless, it is recommended to study the effects of muscle fiber orientation on thin slice measurements in more detail.

The sample preparation was crucial in order to retrieve an accurate and reliable measurement of the unscattered transmittance, which is essential for the correct estimation of both the bulk scattering coefficient and the scattering anisotropy factor (Aernouts et al., 2013; López-Maestresalas et al., 2015). However, this sample preparation involved the cutting of the samples using a cryostat, which proved to be more straightforward for the BF muscle compared to the LL muscle. This might be related to the difference in fiber structure between both muscles (Kirchofer et al., 2002). Moreover, it resulted in a higher number of successful slices for the BF muscle in comparison to the LL muscle. As a result, two slices were obtained for both the OBF and IBF subsamples, while only one slice was retained for the LL subsamples. Overall, this resulted in an equal number of four slices each measurement week for each muscle type, as more LL subsamples per week were considered. However, a higher variation in the results of the LL muscle could be related to the fact that the four slices obtained each week originated from more anatomically different muscle locations in comparison to the OBF and IBF slices. This might explain why some of the observed trends in paragraph 3.3 are not significant. Nevertheless, the general trends in both muscles are similar and in accordance with literature (Xia et al., 2008). In addition, the sample preparation involved a freezing and thawing step. For the freezing of the samples, a rapid freezing using indirect contact with liquid nitrogen was used to minimize the formation of large ice crystals and cracks. However, also the thawing of the samples could have affected the sample (Sen & Sharma, 2004; X. Xia, Kong, Liu, Diao, & Liu, 2012). The thawing of the 0.5 mm thickness slices was performed by adding demineralized water at room temperature. Although small effects of these processing steps might have been present, still

a good agreement was obtained with the results reported by other researchers for studies not including the freezing and thawing of samples (Figure 2).

The evolution of the BOP was investigated at two distinct wavelengths, one related to the absorption of oxymyoglobin and the other related to light scattering. Other wavelengths might be of interest as these relate to the absorption of water, protein content or intramuscular fat. Nevertheless, as demineralized water was added to the samples before measuring, the NIR part of the spectrum is likely to be influenced. For this reason, no evolutions in the NIR region were included in section 3.3.

Besides the optical measurement, the evolution of meat quality traits was also monitored during the wet aging period. The measurement of the WBSF on 10 cylindrical cores of each muscle resulted in a high standard deviation ranging from 7.45 to 24.9 N (Table 1). While a significant decrease in the WBSF values was observed for the LL muscle, the decreasing trend was found to be insignificant for the BF muscle samples. This is in contradiction with the findings of Gruber *et al.* (2006), who reported a significant decrease in the WBSF values for both muscle types. As the measurements in this study were performed on the muscles of only one bull, it is recommended to increase the number of samples and animals in future research. This could confirm the observed trends, both in the reference and optical measurements.

Despite of these shortcomings, the current study provides insights in the BOP of bovine meat samples and their evolution during wet aging. These BOP values provide valuable information for the development and optimization of novel optical sensors for non-destructive quality monitoring in the meat industry. To this end, the obtained BOP values can be used as an input for simulation studies to model the light propagation in order to efficiently evaluate different designs of an optical sensor and novel data processing techniques (Watté et al., 2015a; Watté et al., 2015b). In addition, knowledge on the changes in the interaction of light

509 with muscle tissue during wet aging allows to evaluate the potential of optical measuring
510 systems to monitor meat quality during wet aging.

511

512 ## 5. Conclusions

513 The bulk absorption coefficient, reduced scattering coefficient, bulk scattering coefficient and
514 anisotropy factor spectra of the *longissimus lumborum* (LL) and the *biceps femoris* (BF) were
515 determined at 2, 8 and 16 days postmortem. The BF muscle was further divided into two
516 subgroups, the outer (OBF) and inner BF (IBF), in order to study the effect of two-toning on
517 the estimated optical properties. The absorption coefficient showed distinct absorption
518 features of myoglobin at 544 nm and 582 nm, and of water at 970 nm, 1200 nm and 1450
519 nm. Moreover, it was found that the BF expressed a significantly higher absorption in the
520 visible range of the spectrum, attributed to myoglobin, compared to the LL muscle. However,
521 no significant difference was found between the OBF and IBF samples. Furthermore, the
522 reduced scattering coefficient was significantly higher for the IBF muscle over the entire
523 wavelength range measured. This difference was mainly caused by a significantly lower
524 anisotropy factor for the BF muscle. In addition, the anisotropy factor for both muscles was
525 close to 1, indicating a high forward scattering, with mean values of up to 0.96 at 800 nm for
526 the LL muscle. Clear differences between the IBF and OBF samples were found for all
527 scattering properties. It was hypothesized that these may have been caused by an increased
528 degree of protein denaturation in the IBF samples, due to a faster post-mortem pH decline.
529 As no difference in absorption was observed between the OBF and IBF samples, the visual
530 effect of two-toning is mainly related to light scattering. During wet aging, a significant
531 decrease in the measured anisotropy factor was noticed in both the LL and IBF samples.
532 During the same period, the LL tenderness increased. Both observations are most likely
533 related to the proteolysis of cytoskeletal proteins during the wet aging period.

This study provides novel insights in the relation between the bulk optical properties and the quality attributes of bovine meat samples during wet aging. This information is essential for understanding light propagation in bovine muscle tissue and to optimize data processing algorithms and innovative optical sensors for meat quality monitoring.

Acknowledgements

Robbe Van Beers was funded by the Institute for the Promotion of Innovation through Science and Technology in Flanders (IWT-Flanders, grant number 131777). Mito Kokawa was funded as a postdoctoral fellow of the Japan Society for the Promotion of Science (JSPS). Ben Aernouts was funded as a postdoctoral fellow of the Research Foundation Flanders (FWO, Brussels, Belgium, grant number 12K3916N). Md. Hafizur Rahman Bhuyian is acknowledged for his valuable exploratory work in determining the BOP of beef samples. Lut Noterdaeme and Pieter Vancamp, from the KU Leuven division of animal physiology and neurobiology, are acknowledged for their advice and assistance in preparing the samples slices with the microtome-cryostat. The authors would also like to thank the commercial meat handling facility Hemelaer-NV in Belgium for providing the meat samples.

6. References

Aernouts, B., Van Beers, R., Watté, R., Huybrechts, T., Jordens, J., Vermeulen, D., … Saeys, W. (2015). Effect of ultrasonic homogenization on the Vis/NIR bulk optical properties of milk. *Colloids and Surfaces B: Biointerfaces*, *126*, 510–519. http://doi.org/10.1016/j.colsurfb.2015.01.004

Aernouts, B., Van Beers, R., Watté, R., Huybrechts, T., Lammertyn, J., & Saeys, W. (2015). Visible and near-infrared bulk optical properties of raw milk. *Journal of Dairy Science*, *98*(7), 6727–6738. http://doi.org/10.3168/jds.2015-9630

Aernouts, B., Zamora-Rojas, E., Van Beers, R., Watté, R., Wang, L., Tsuta, M., … Saeys, W. (2013). Supercontinuum laser based optical characterization of Intralipid® phantoms in the 500-2250 nm range. *Optics Express*, *21*(26), 32450–67. http://doi.org/10.1364/OE.21.032450

Bashkatov, A. N., Genina, E. A., Kochubey, V. I., & Tuchin, V. V. (2005). Optical properties of human skin, subcutaneous and mucous tissues in the wavelength range from 400 to 2000 nm. *Journal of Physics D: Applied Physics*, *38*(15), 2543–2555. http://doi.org/10.1088/0022-3727/38/15/004

Boccard, R., Buchter, L., Casteels, E., Cosentino, E., Dransfield, E., Hood, D. ., … Touraille, C. (1981). Procedures for measuring meat quality characteristics in beef production experiments. Report of a working group in the commission of the European communities' (CEC) beef production research programme. *Livestock Production Science*, *8*(5), 385–397. http://doi.org/10.1016/0301-6226(81)90061-0

Bratcher, C. L., Johnson, D. D., Littell, R. C., & Gwartney, B. L. (2005). The effects of quality grade, aging, and location within muscle on Warner–Bratzler shear force in beef muscles of locomotion. *Meat Science*, *70*(2), 279–284. http://doi.org/http://dx.doi.org/10.1016/j.meatsci.2005.01.013

Cozzolino, D., & Murray, I. (2004). Identification of animal meat muscles by visible and near infrared reflectance spectroscopy. *LWT - Food Science and Technology*, *37*(4), 447–452. http://doi.org/10.1016/j.lwt.2003.10.013

Damez, J.-L., & Clerjon, S. (2013). Quantifying and predicting meat and meat products quality attributes using electromagnetic waves: An overview. *Meat Science*, *95*(4), 879–896. http://doi.org/10.1016/j.meatsci.2013.04.037

Damez, J. L., & Clerjon, S. (2008). Meat quality assessment using biophysical methods related to meat structure. *Meat Science*, *80*(1), 132–149. http://doi.org/10.1016/j.meatsci.2008.05.039

Dirckx, J., Kuypers, L., & Decraemer, W. (2005). Refractive index of tissue measured with confocal microscopy. *J. Biomed. Opt.* http://doi.org/10.1117/1.1993487

Elliott, R. J. (1967). EFFECT OF OPTICAL SYSTEMS AND SAMPLE PREPARATION ON THE VISIBLE REFLECTION SPECTRA OF PORK MUSCLE. *J. Sci. Fd Agric.*, *18*(August), 332–338.

Elmasry, G., Sun, D. W., & Allen, P. (2012). Near-infrared hyperspectral imaging for predicting colour, pH and tenderness of fresh beef. *Journal of Food Engineering*, *110*(1), 127–140. http://doi.org/10.1016/j.jfoodeng.2011.11.028

Flock, S. T., Wilson, B. C., & Patterson, M. S. (1987). Total attenuation coefficients and scattering phase functions of tissues and phantom materials at 633 nm. *Medical Physics*, *14*(5), 835–841. http://doi.org/10.1118/1.596010

Gruber, S. L., Tatum, J. D., Scanga, J. A., Chapman, P. L., Smith, G. C., & Belk, K. E. (2006). Effects of postmortem aging and USDA quality grade on Warner-Bratzler shear force values of seventeen individual beef muscles. *Journal of Animal Science*, *84*(12), 3387–3396. http://doi.org/10.2527/jas.2006-194

Hale, G. M., & Querry, M. R. (1973). Optical Constants of Water in the 200-nm to 200-µm Wavelength Region. *Applied Optics*, *12*(3), 555–563. http://doi.org/10.1364/AO.12.000555

Jacques, S. L. (2013). Optical Properties of Biological Tissues: A Review. *Physics in*

603 *Medicine and Biology*, *58*(11), R37-61. http://doi.org/10.1088/0031-9155/58/11/R37
604 Jeremiah, L. E., & Gibson, L. L. (2003). The effects of postmortem product handling and
605 aging time on beef palatability. *Food Research International*, *36*(9–10), 929–941.
606 http://doi.org/http://dx.doi.org/10.1016/S0963-9969(03)00102-9
607 Kauffman, R. G., Habel, R. E., Smulders, F. J. M., Hartman, W., & Bergström, P. L. (1990).
608 Recommended terminology for the muscle commonly designated “Longissimus dorsi.”
609 *Meat Science*, *28*, 259–265.
610 Kienle, A., Foschum, F., & Hohmann, A. (2013). Light propagation in structural anisotropic
611 media in the steady-state and time domains. *Physics in Medicine and Biology*, *58*,
612 6205–23. http://doi.org/10.1088/0031-9155/58/17/6205
613 Kirchofer, K. S., Calkins, C. R., & Gwartney, B. L. (2002). Fiber-type composition of muscles
614 of the beef chuck and round. *Journal of Animal Science*, *80*, 2872–2878.
615 Koohmaraie, M. (1994). Muscle proteinases and meat aging. *Meat Science*, *36*(1–2), 93–
616 104. http://doi.org/http://dx.doi.org/10.1016/0309-1740(94)90036-1
617 Leffler, T. P., Moser, C. R., McManus, B. J., Urh, J. J., Keeton, J. T., Claflin, A., … Steiner,
618 G. (2008). Determination of moisture and fat in meats by microwave and nuclear
619 magnetic resonance analysis: Collaborative study. *Journal of AOAC International*, *91*(4),
620 802–810.
621 Li, C., Zhou, G., & Xu, X. (2008). Changes of meat quality characteristics and intramuscular
622 connective tissue of beef semitendinosus muscle during postmortem aging for Chinese
623 Yellow bulls. *International Journal of Food Science and Technology*, *43*(5), 838–845.
624 http://doi.org/10.1111/j.1365-2621.2007.01524.x
625 López-Maestresalas, A., Aernouts, B., Van Beers, R., Arazuri, S., Jarén, C., de
626 Baerdemaeker, J., & Saeys, W. (2015). Bulk Optical Properties of Potato Flesh in the
627 500–1900 nm Range. *Food and Bioprocess Technology*, *9*(3), 463–470.
628 http://doi.org/10.1007/s11947-015-1639-0
629 MacDougall, D. B. (1982). Changes in the colour and opacity of meat. *Food Chemistry*, *9*(1–
630 2), 75–88. http://doi.org/10.1016/0308-8146(82)90070-X
631 Mager, S. R., Oomen, M. H. A., Morente, M. M., Ratcliffe, C., Knox, K., Kerr, D. J., …
632 Riegman, P. H. J. (2007). Standard operating procedure for the collection of fresh
633 frozen tissue samples. *European Journal of Cancer*, *43*(5), 828–834.
634 http://doi.org/10.1016/j.ejca.2007.01.002
635 Millar, S. J., Moss, B. W., & Stevenson, M. H. (1996). Some observations on the absorption
636 spectra of various myoglobin derivatives found in meat. *Meat Science*, *42*(3), 277–288.
637 http://doi.org/10.1016/0309-1740(94)00045-X
638 Nicolaï, B. M., Beullens, K., Bobelyn, E., Peirs, A., Saeys, W., Theron, K. I., & Lammertyn, J.
639 (2007). Nondestructive measurement of fruit and vegetable quality by means of NIR
640 spectroscopy: A review. *Postharvest Biology and Technology*, *46*(2), 99–118.
641 http://doi.org/10.1016/j.postharvbio.2007.06.024
642 Nicolaï, B. M., Defraeye, T., De Ketelaere, B., Herremans, E., Hertog, M. L. a T. M., Saeys,
643 W., … Verboven, P. (2014). Nondestructive measurement of fruit and vegetable quality.
644 *Annual Review of Food Science and Technology*, *5*, 285–312.
645 http://doi.org/10.1146/annurev-food-030713-092410
646 Pastsart, U., De Boever, M., Claeys, E., & De Smet, S. (2013). Effect of muscle and post-
647 mortem rate of pH and temperature fall on antioxidant enzyme activities in beef. *Meat*
648 *Science*, *93*(3), 681–686. http://doi.org/10.1016/j.meatsci.2012.11.008
649 Pastsart, U., De Boever, M., Lescouhier, S., Claeys, E., & De Smet, S. (2011). Effect of Hot
650 Boning on Colour Stability and Antioxidant Enzyme Activities in Beef Inner and Outer
651 Biceps femoris. In *57 th International Congress of Meat Science and Technology* (p.
652 243).
653 Peng, Y., & Dhakal, S. (2015). Optical Methods and Techniques for Meat Quality Inspection.
654 *Transactions of the ASABE*, *58*(5), 1371–1386. http://doi.org/10.13031/trans.58.11004
655 Prahl, S. (2011). Everything I think you should know about Inverse Adding-Doubling. *Oregon:*
656 *Oregon Medical Laser Center, St. Vincent Hospital.*, 1–74.
657 Prahl, S. A., van Gemert, M. J. C., & Welch, A. J. (1993). Determining the optical properties

658 of turbid mediaby using the adding-doubling method. *Applied Optics*, *32*(4), 559–568.
659 http://doi.org/10.1364/AO.32.000559
660 Prieto, N., Roehe, R., Lavín, P., Batten, G., & Andrés, S. (2009). Application of near infrared
661 reflectance spectroscopy to predict meat and meat products quality: A review. *Meat*
662 *Science*, *83*(2), 175–86. http://doi.org/10.1016/j.meatsci.2009.04.016
663 Prieto, N., Ross, D. W., Navajas, E. A., Nute, G. R., Richardson, R. I., Hyslop, J. J., …
664 Roehe, R. (2009). On-line application of visible and near infrared reflectance
665 spectroscopy to predict chemical–physical and sensory characteristics of beef quality.
666 *Meat Science*, *83*(1), 96–103. http://doi.org/10.1016/j.meatsci.2009.04.005
667 Ranasinghesagara, J., & Yao, G. (2007). Imaging 2D optical diffuse reflectance in skeletal
668 muscle. *Optics Express*, *15*(7), 3998–4007. http://doi.org/10.1364/OE.15.003998
669 Rhee, M. S., Wheeler, T. L., Shackelford, S. D., & Koohmaraie, M. (2004). Variation in
670 palatability and biochemical traits within and among eleven beef muscles. *Journal of*
671 *Animal Science*, *82*(2), 534–550. http://doi.org//2004.822534x
672 Rickansrud, D. A., & Henrickson, R. L. (1967). Total Pigments and Myoglobin Concentration
673 In Four Bovine Muscles. *Journal of Food Science*, *32*(1), 57–61.
674 http://doi.org/10.1111/j.1365-2621.1967.tb01957.x
675 Ripoll, G., Albertí, P., Panea, B., Olleta, J. L., & Sañudo, C. (2008). Near-infrared reflectance
676 spectroscopy for predicting chemical, instrumental and sensory quality of beef. *Meat*
677 *Science*, *80*(3), 697–702. http://doi.org/10.1016/j.meatsci.2008.03.009
678 Rowe, P. I., Künnemeyer, R., McGlone, A., Talele, S., Martinsen, P., & Seelye, R. (2014).
679 Relationship between tissue firmness and optical properties of “Royal Gala” apples from
680 400 to 1050nm. *Postharvest Biology and Technology*, *94*, 89–96.
681 Saeys, W., Velazco-Roa, M. a, Thennadil, S. N., Ramon, H., & Nicolaï, B. M. (2008). Optical
682 properties of apple skin and flesh in the wavelength range from 350 to 2200 nm. *Applied*
683 *Optics*, *47*(7), 908–19.
684 Sen, A. R., & Sharma, N. (2004). Effect of freezing and thawing on the histology and
685 ultrastructure of buffalo muscle. *Asian-Australasian Journal of Animal Sciences*, *17*(9),
686 1291–1295.
687 Smith, R. D., Nicholson, K. L., Nicholson, J. D. W., Harris, K. B., Miller, R. K., Griffin, D. B., &
688 Savell, J. W. (2008). Dry versus wet aging of beef: Retail cutting yields and consumer
689 palatability evaluations of steaks from US Choice and US Select short loins. *Meat*
690 *Science*, *79*(4), 631–639. http://doi.org/10.1016/j.meatsci.2007.10.028
691 Swartling, J., Dam, J. S., & Andersson-Engels, S. (2003). Comparison of spatially and
692 temporally resolved diffuse-reflectance measurement systems for determination of
693 biomedical optical properties. *Applied Optics*, *42*(22), 4612–20. Retrieved from
694 http://www.ncbi.nlm.nih.gov/pubmed/12916630
695 Swatland, H. J. (1991). Spatial and Spectrophotometric Measurements of Light Scattering in
696 Turkey Breast Meat Using Lasers and a Xenon Arc. *Canadian Institute of Food Science*
697 *and Technology Journal*, *24*(1–2), 27–31. http://doi.org/10.1016/S0315-5463(91)70015-
698 1
699 Swatland, H. J. (1994). Physical measurements of meat quality: optical measurements, pros
700 and cons. *Meat Science*, *36*(1–2), 251–9. http://doi.org/10.1016/0309-1740(94)90044-2
701 Swatland, H. J. (2004). Progress in understanding the paleness of meat with a low pH. *South*
702 *African Journal of Animal Sciences*, *34*(6SUPPL.2), 1–7.
703 Troy, D. J., & Kerry, J. P. (2010). Consumer perception and the role of science in the meat
704 industry. *Meat Science*, *86*(1), 214–226. http://doi.org/10.1016/j.meatsci.2010.05.009
705 Tuchin, V. (2007). Methods and algorithms for the measurements of optical parameters of
706 tissues. In *Tissue Optics* (Second Edi, pp. 143–256). Bellingham, WA: SPIE Press.
707 Van Beers, R., Aernouts, B., León Gutiérrez, L., Erkinbaev, C., Rutten, K., Schenk, A., …
708 Saeys, W. (2015). Optimal Illumination-Detection Distance and Detector Size for
709 Predicting Braeburn Apple Maturity from Vis/NIR Laser Reflectance Measurements.
710 *Food and Bioprocess Technology*, *8*(10), 2123–2136. http://doi.org/10.1007/s11947-
711 015-1562-4
712 Van Beers, R., Aernouts, B., Reis, M. M., & Saeys, W. (2017). Anisotropic light propagation

713 in bovine muscle tissue depends on the initial fiber orientation, muscle type and
714 wavelength. *Optics Express*, *25*(18), 22082–22095.
715 http://doi.org/10.1364/OE.25.022082
716 Van Beers, R., Aernouts, B., Watté, R., Schenk, A., Nicolaï, B., & Saeys, W. (2017). Effect of
717 maturation on the bulk optical properties of apple skin and cortex in the 500 to 1850 nm
718 wavelength range. *Journal of Food Engineering*, *Submitted*.
719 Van Oeckel, M. J., Warnants, N., & Boucqué, C. V. (1999). Measurment and prediction of
720 pork colour. *Meat Science*, *52*, 347–354.
721 Von Seggern, D. D., Calkins, C. R., Johnson, D. D., Brickler, J. E., & Gwartney, B. L. (2005).
722 Muscle profiling: Characterizing the muscles of the beef chuck and round. *Meat*
723 *Science*, *71*(1), 39–51. http://doi.org/10.1016/j.meatsci.2005.04.010
724 Wang, W., & Li, C. (2013). Measurement of the light absorption and scattering properties of
725 onion skin and flesh at 633nm. *Postharvest Biology and Technology*, *86*, 494–501.
726 http://doi.org/10.1016/j.postharvbio.2013.07.032
727 Watté, R., Aernouts, B., Van Beers, R., Herremans, E., Ho, Q. T., Verboven, P., … Saeys,
728 W. (2015). Modeling the propagation of light in realistic tissue structures with MMC-fpf: a
729 meshed Monte Carlo method with free phase function. *Optics Express*, *23*(13), 17467.
730 http://doi.org/10.1364/OE.23.017467
731 Watté, R., Aernouts, B., Van Beers, R., Postelmans, A., & Saeys, W. (2016). Computational
732 optimization of the configuration of a spatially resolved spectroscopy sensor for milk
733 analysis. *Analytica Chimica Acta*, *917*, 53–63. http://doi.org/10.1016/j.aca.2016.02.041
734 Xia, J. J., Berg, E. P., Lee, J. W., & Yao, G. (2007). Characterizing beef muscles with optical
735 scattering and absorption coefficients in VIS-NIR region. *Meat Science*, *75*(1), 78–83.
736 Xia, J., Weaver, A., Gerrard, D. E., & Yao, G. (2008). Distribution of optical scattering
737 properties in four beef muscles. *Sensing and Instrumentation for Food Quality and*
738 *Safety*, *2*(2), 75–81.
739 Xia, X., Kong, B., Liu, J., Diao, X., & Liu, Q. (2012). Influence of different thawing methods on
740 physicochemical changes and protein oxidation of porcine longissimus muscle. *LWT -*
741 *Food Science and Technology*, *46*(1), 280–286. http://doi.org/10.1016/j.lwt.2011.09.018
742 Yavari, N. (2006). *Optical spectroscopy for tissue diagnostics and treatment control*. *Doctoral*
743 *Thesis*. Retrieved from http://bora.uib.no/handle/1956/1684
744 Zamora-Rojas, E., Aernouts, B., Garrido-Varo, A., Pérez-Marín, D., Guerrero-Ginel, J. E., &
745 Saeys, W. (2013). Double integrating sphere measurements for estimating optical
746 properties of pig subcutaneous adipose tissue. *Innovative Food Science & Emerging*
747 *Technologies*, *19*, 218–226.
748 Zamora-Rojas, E., Garrido-Varo, A., Aernouts, B., Pérez-Marín, D., Saeys, W., Yamada, Y.,
749 & Guerrero-Ginel, J. E. (2014). Understanding near infrared radiation propagation in pig
750 skin reflectance measurements. *Innovative Food Science and Emerging Technologies*,
751 *22*, 137–146. http://doi.org/10.1016/j.ifset.2014.01.006
752 Zijp, J. R., & ten Bosch, J. J. (1998). Optical properties of bovine muscle tissue in vitro; a
753 comparison of methods. *Physics in Medicine and Biology*, *43*, 3065–3081.
754